IPT9, a cis-zeatin cytokinin biosynthesis gene, promotes root growth

Ioanna Antoniadi[1†*], Eduardo Mateo-Bonmatí[1,6†], Markéta Pernisová[2‡], Federica Brunoni[1,3‡], Mariana Antoniadi[1], Mauricio Garcia-Atance Villalonga[4], Anita Ament[3], Michal Karády[3], Colin Turnbull[4], Karel Doležal[3,5], Ales Pěnčík[3], Karin Ljung[1], and Ondřej Novák[1,3*]

[1]Umeå Plant Science Centre, Department of Forest Genetics and Plant Physiology, Swedish University of Agricultural Sciences, SE-901 83 Umeå, Sweden.
[2]Plant Sciences Core Facility, Mendel Centre for Plant Genomics and Proteomics, Central European Institute of Technology (CEITEC), and NCBR, Faculty of Science, Masaryk University, CZ-62500 Brno, Czech Republic.
[3]Laboratory of Growth Regulators, Institute of Experimental Botany of the Czech Academy of Sciences and Faculty of Science of Palacký University, CZ-78371 Olomouc, Czech Republic.
[4]Department of Life Sciences, Imperial College London, London SW7 2AZ, United Kingdom.
[5]Department of Chemical Biology, Faculty of Science, Palacký University, CZ-78371 Olomouc, Czech Republic
[6]Current address: John Innes Centre, NR4 7UA, Norwich, United Kingdom.

[†]*These authors have contributed equally to this work as first authors*
[‡]*These authors have contributed equally to this work as second authors*

*****Correspondence to:
Ioanna Antoniadi: ioanna.antoniadi@slu.se and,
Ondrej Novak: novako@ueb.cas.cz

Keywords (5-8): Cytokinin, auxin, metabolism, plant hormone, root growth

Running title (5 words max): IPT9 promotes root growth.

Word count (total): 10504
Abstract: 257; Introduction: 1069; Methods: 1388; Results: 1632 ;Discussion: 2014; Legends: 671, References: 2929.

Figures: 5

Tables: 0

Supplementary Figures: 3

Supplementary Tables: 1

ABSTRACT

Cytokinin and auxin are plant hormones that coordinate many aspects of plant development. Their interactions in plant underground growth are well established, occurring at the levels of metabolism, signaling, and transport. Unlike many plant hormone classes, cytokinins are represented by more than one active molecule. Multiple mutant lines, blocking specific parts of cytokinin biosynthetic pathways, have enabled research in plants with deficiencies in specific cytokinin-types. While most of these mutants have confirmed the impeding effect of cytokinin on root growth, the *ipt29* double mutant instead surprisingly exhibits reduced primary root length compared to wild type. This mutant is impaired in *cis*-zeatin (*c*Z) production, a cytokinin-type that had been considered inactive in the past. Here we have further investigated the intriguing *ipt29* root phenotype, opposite to known cytokinin functions, and the (bio)activity of *c*Z. Our data suggest that despite the *ipt29* short-root phenotype, *c*Z application has a negative impact on primary root growth and can activate a cytokinin response in the stele. Grafting experiments revealed that the root phenotype of *ipt29* depends on local signaling which does not relate to directly to cytokinin levels. Notably, *ipt29* displayed increased auxin levels in the root tissue. Moreover, analyses of the differential contributions of *ipt2* and *ipt9* to the *ipt29* short-root phenotype demonstrated that, despite its deficiency on *c*Z levels, *ipt2* does not show any root phenotype or auxin homeostasis variation while *ipt9* mutants were indistinguishable from *ipt29*. We conclude that IPT9 functions may go beyond *c*Z biosynthesis, directly or indirectly, implicating effects on auxin homeostasis and therefore influencing plant growth.

INTRODUCTION

Plant roots are a highly powerful and dynamic part of the plant body that builds its underground architecture in search of water, anchorage and nourishment. Thus, the regulation of root growth and development is essential to plant prosperity and to their adaptability in changing environmental conditions. Cytokinins (CKs) have been long known inhibitors of root growth and development (1) and multiple mutants blocking CK biosynthesis, display enhanced primary root length compared to the wild type plants (2). In the past, *cis*-zeatin (*c*Z)-forms of cytokinin (CK) were considered less important than isopentenyl adenine (iP) and *trans*-zeatin (*t*Z)-forms due to their weaker responses in some bioassays (3,4) but also due to lack of research on them. More recently, it has been shown that *c*Z can be perceived by CK receptors in *Arabidopsis thaliana* (hereafter, Arabidopsis) and *Zea mays* (hereafter, maize; (5–8)) and that they are also bioactive in several assays (9). *c*Z-types were also detected as the main CK compound in developing seeds of chickpeas (*Cicer arietinum;* (10)), in all tissues of maize (11), in the flag leaves of rice (*Oryza sativa;* (12)) and during embryogenesis of pea (*Pisum sativum;* (13)). Additional evidence for *c*Z activity were presented when enzymes responsible for zeatin-O-glucosides production showed striking preference in *c*Z conjugation in maize (11). Similarly, the *c*Z-O-glucosyltransferases (*c*ZOGT1,2,3) identified in rice preferentially catalyze O-glucosylation of *c*Z-CKs than *t*Z-CKs (14). The suggestion that *c*Z has physiological effects on plant development was based on the phenotypes of *c*ZOGT overexpressor lines in rice, which displayed defects in crown root numbers, leaf senescence and shoot size (14). The direct impact of *c*Z activity in root elongation impairment was also exhibited *in tandem* with upregulation of CK response genes in rice (14). Salinity stress caused fast accumulation of *c*Z and the *c*Z precursor, *c*ZR (*cis*-zeatin riboside) in maize roots, while no change was observed in *t*Z levels (15). Similar increases in *c*Z-types were also observed following drought (16), heat (17) and biotic stress (18). In addition, a biological role for *c*Z-types in the regulation of xylem specification was recently reported (19). However, even though the double mutant of tRNA-AtIPTs, *ipt29*, had undetectable levels of all *c*Z-types, it displayed only chlorotic phenotype and was otherwise developmentally normal (2). Overall, *c*Z-types have been detected in more than 150 plant species and regardless their evolutionary complexity (9).

CK biosynthesis is catalyzed by 9 isopentenyl transferase enzymes (IPTs) in Arabidopsis (2). IPT1 and IPT3-8 are responsible for isopentenyl adenine (iP) and *t*Z compounds production (2). The biosynthesis of the latter ones requires an additional carboxylation step catalyzed by two cytochrome P450 enzymes (CYP735A1 and CYP735A2) (20,21). In parallel, IPT2 and IPT9 are responsible for *c*Z-type production following tRNA degradation (2). CK compounds can be categorized in two ways: (1) according to their side chain modifications (iP-, *t*Z- and *c*Z-

compounds), and (2) to the changes in their adenine molecule during their metabolism (the precursor forms: phosphates and ribosides, the active free bases and the catabolite products: *N*- and *O*-glucosides (reviewed in (22)). The participation of *c*Z-compounds in CK homeostatic mechanism was demonstrated by the unanimous increased concentrations of *c*Z-types when *t*Z-types were deficient, in *ipt1 ipt3 ipt5 ipt7* (*ipt1357*) and *cyp735a1 cyp735a1a2* (*cypa1a2*) multiple mutants (20,23) and in *abcg14* (24,25). Interestingly, *c*Z-CK levels were increased in the mutants mentioned above only when *t*Z-types levels were reduced but not iP-types. The identification of *c*ZR as a major transport form of CK could also contribute to maintenance of CK homeostasis in the shoots (26).

The active CK molecules, free bases, are perceived by hybrid histidine kinases (HKs) in the CK-responsive cells and transcription is activated via a phospho-relay signaling cascade (27). The final step of this signaling network involves type-B nuclear RESPONSE REGULATOR (B-RR) proteins that mediate transcriptional activation by binding to promoters of immediate-early target genes via a conserved Myb-related DNA-binding domain. Global RR-B transcriptional activity and thus *in vivo* monitoring of these CK-dependent transcriptional responses, can be facilitated by the CK-responsive synthetic reporter *TCSn::GFP* expression in Arabidopsis plants (28). The signal output of this reporter line has also been shown to reflect CK content (29).

Although CK plays a pivotal role in root growth and development, several studies have shown that appropriate plant underground growth also depends on CK cross-talks with other phytohormones, such as indole-3-acetic acid (IAA), the main auxin. Derived from the amino acid L-Tryptophan (Trp), parallel biosynthetic and inactivation pathways converge to control IAA concentration (30). The main biosynthetic route, deaminates Trp to indole-3-pyruvic acid (IPyA) which is then decarboxylated to IAA. Although not completely clear, other routes exist connecting IAA biosynthesis with defensive compounds (glucosinolates) via indole acetaldoxime (IAOx). It has been hypothesized that IAOx, is then converted to indole acetonitrile (IAN) which is finally transformed into IAA. IAA levels are also controlled by redundant inactivation mechanisms including conjugation to sugars catalysed by different UGTs (42), GH3-driven conjugation to amino acids (43,44), and oxidation via DAO enzymes (45,46).

In this work, we monitored the primary root growth of three multiple mutant lines *ipt357*, *cypa1a2* and *ipt29*, which have impeded production of iP-, *t*Z- and *c*Z-type compounds, respectively. While *ipt357* and *cypa1a2* enhanced root growth is in agreement with the inhibitory effect of CKs on primary root growth, *ipt29* roots displayed severe retardation compared to wild type root length as also previously reported (19). We therefore investigated further the *ipt29* root phenotype, opposite to CK known functions, and the (bio)activity of *c*Z in the root tip. Our results showed that

in spite of the defective growth of *ipt29* root, exogenous application of *c*Z triggers CK responses in the root vasculature and halts primary root growth. In parallel, grafting experiments indicated that *ipt29* root phenotype relies mainly on local signaling. Since this root signal was proven to be CK-independent, we examined auxin as a possible candidate, finding enhanced auxin levels the roots of *ipt29*. Finally, we analysed the differential contribution of *ipt2* and *ipt9* to the short-root phenotype. Surprisingly, even though there was a remarkable effect on *c*Z levels, *ipt2* root length and IAA levels were found normal while the *ipt9* single mutant showed a strong root phenotype and IAA levels indistinguishable from *ipt29*. No additional insertions in *ipt9* were found by genome-wide sequencing, and complementation tests and transgenic overexpression further confirmed the link between the short root phenotype and lesions in *IPT9*. Our data suggests that IPT9 bifunctionally works on *c*Z and IAA homeostasis and promotes root growth.

MATERIALS AND METHODS

Plant material, culture conditions and root phenotyping

Unless otherwise stated, all *Arabidopsis thaliana* plants studied in this work were homozygous for the mutations indicated. Single mutants *ipt2* (2), *ipt9-1* (2) multiple mutant *ipt357* (2), *cypa1a2* (20), *ipt29* (2), and the transgenic reporter line *TCSn::GFP* (28), *ARR5*$_{pro}$*:GUS* (55), all in Col-0 background, were previously described. The Nottingham Arabidopsis Stock Centre provided seeds for the wild-type accession Col-0 (N1092), and *ipt9-2* (GABI_302F10; N428966).

The presence and position of all insertions were confirmed by PCR amplification using gene-specific primers, together with insertion-specific primers (Supplemental Table 1). In all experiments the seeds were surface sterilised with 20% (v/v) dilution of bleach for 5 min (2 × 2.5 min) and then rinsed five times with sterile water before sown under sterile conditions on Petri dishes containing half-strength Murashige and Skoog agar medium with 1% of sucrose. Stratification occurred at 4ºC for 3 days and then plates were transferred to light at 22 ± 1°C where the seedlings grew for 7 days under cool white fluorescent light (maximum irradiance 150 µmol m^{-2} s^{-1}). For primary root length phenotyping the plates were scanned with Epson Perfection V600 Photo. Length quantifications were performed using FIJI software (56).

Seedling treatments

Plants were grown in the above-described solid media supplemented with 100 nM of iP, *t*Z and *c*Z (Olchemim), respectively. After 7 days the plates were scanned and the root length was measured. For the root elongation assay, the seedlings were grown for 6 days in hormone-free media (as described in the previous section) prior to transfer to the media supplemented with 100

nM iP, *tZ* and *cZ*, under sterile conditions. The seedlings' root tip positions were marked on the plates and they were returned to the growth chamber for 24h. After that, the plates were scanned and root elongation was measured.

Histochemical staining

ARR5$_{pro}$:GUS seedlings were stained in 0.1 M sodium phosphate buffer (pH 7.0) containing 0.1% X-GlcA sodium salt (Duchefa), 1 mM $K_3[Fe(CN)_6]$, 1 mM $K_4[Fe(CN)_6]$ and 0.05% Triton X-100 for 30 minutes at 37°C and were incubated overnight in 80% (vol/vol) ethanol at room temperature. Tissue clearing was conducted as previously described in (57).

Microscopy

GFP expression patterns in 7-day-old *TCSn::GFP* seedlings was recorded using confocal laser scanning microscopy (Zeiss LSM800). The 488 nm laser line was employed for the GFP fluorescence detection, and emission was detected between 490 and 580 nm. Two tile scans were performed for root imaging. DIC microscopy was performed on an Olympus BX61 microscope equipped with ×10 and ×20 air objectives and a DP70 CCD camera.

Auxin and Cytokinin measurements

Wild type and mutant plant roots were excised after 7 days of growth. The tissue was weighted and snap frozen in liquid nitrogen until hormone purification and analysis when frozen samples were thawed on ice.

For CKs analysis, samples (10 mg fresh weight) were homogenized and extracted in 0.5 ml of modified Bieleski buffer (60% MeOH, 10% HCOOH and 30% H_2O) together with a cocktail of stable isotope-labelled internal standards used as a reference (0.25 pmol of CK bases, ribosides, N-glucosides, and 0.5 pmol of CK O-glucosides, nucleotides per sample added). CKs were purified using in-tip solid-phase microextraction based on the StageTips technology as described previously (58). Briefly, combined multi-StageTips (containing C18/SDB-RPSS/Cation-SR layers) were activated sequentially with 50 µl each of acetone, methanol, water, 50% (v/v) nitric acid and water (by centrifugation at 434×*g*, 15 min, 4 °C). After application of the sample (500 µl, 678×*g*, 30 min, 4 °C), the microcolumns were washed sequentially with 50 µl of water and methanol (525×*g*, 20 min, 4 °C), and elution of samples was performed with 50 µl of 0.5M NH4OH in 60% (v/v) methanol (525×*g*, 20 min, 4 °C). The eluates were then evaporated to dryness *in vacuo* and stored at −20 °C. The CK profile was then quantitatively analysed by multiple reaction monitoring using an ultra-high performance liquid chromatography-electrospray tandem mass spectrometry

(UHPLC-MS/MS). Separation was performed on an Acquity UPLC i-Class System (Waters, Milford, MA, USA) equipped with an Acquity UPLC BEH Shield RP18 column (150x2.1 mm, 1.7 µm; Waters), and the effluent was introduced into the electrospray ion source of a triple quadrupole mass spectrometer Xevo TQ-S MS (Waters).

Analysis of endogenous IAA precursors and metabolites was performed using the method described in (59). Briefly, approx. 2.5 mg of roots or 10 mg of shoots were extracted in 50 mM phosphate buffer (pH 7.0) containing 0.1% sodium diethyldithiocarbamate and stable isotope-labelled internal standards. 200 µl portion of each extract was acidified with 1M HCl to pH 2.7 and purified by in-tip micro solid phase extraction (in-tip µSPE). For quantification of IPyA, the second 200 µl portion of the extract was derivatized by cysteamine (0.75 M, pH 8.2) for 15 minutes, acidified with 3M HCl to pH 2.7 and purified by in-tip µSPE. After evaporation under reduced pressure, samples were analyzed using HPLC system 1260 Infinity II (Agilent Technologies, Santa Clara, CA, USA) equipped with Kinetex C18 (50 mm x 2.1 mm, 1.7 µm; Phenomenex Torrance, CA, USA). The LC system was linked to 6495 Triple Quad mass spectrometer (Agilent Technologies).

CK and auxin concentrations were determined using MassLynx software (v4.2; Waters) and Mass Hunter software (version B.05.02; Agilent Technologies), respectively, using stable isotope dilution method. At least four independent biological replicates were performed, including two technical replicates of each.

Grafting Experiments

Plants were grown vertically on 100 mm square plates containing 25 ml of 1/2 MS growth media at pH 5.7. Seeds (10 mg) were added to a 1.5ml Eppendorf tube with 1 ml of 70% ethanol and shaken at 21°C for 30 seconds. After washing with 1 ml of milliQ water, seeds were surface sterilised for 6 minutes in 1 ml of 1:10 diluted bleach, then washed six times with 1 ml of milliQ water. A 200 µl Gilson pipette was then used to suck up one seed at a time and transfer it on to plates, that were then kept at 4°C for 48 hours for stratification. The plates were then transferred to a controlled environment room at 23°C with a 16 hour photoperiod. After 5 days, plates were placed in a lit cupboard at 27°C. At 6 days post-stratification, simple hypocotyl grafting without a supporting collar was performed according to Turnbull et al. 2002. The non-grafted, self-grafted and trans-grafted seedlings were placed again at 27°C for another 4 days, then transferred back to 23°C. The plants were checked every day for evidence of contamination and to eliminate any adventitious roots growing above the grafting incision. This was carried out causing minimum

disturbance to allow for graft union formation (60). Eight days post grafting the plates were scanned and the root length was measured in all successful grafts.

Transgene complementation

To construct the *35S$_{pro}$:IPT9*, the At5g20040 transcription unit was amplified from Col-0 cDNA using the Q5 High-Fidelity DNA Polymerase (NEB), as recommended by the manufacturer using the oligonucleotides attB_IPT9_F and attB_IPT9_R, that contained attB sites at their 5' ends (Supplemental Table 1). The PCR product obtained were purified using the Monarch DNA Gel Extraction Kit (NEB) and cloned into the pDONR207 using a BP Clonase II Kit (Thermo Fisher). Chemically competent *Escherichia coli* DH5α cells were transformed by the heat-shock method (Dagert and Ehrlich 1979), and the structural integrity of the inserts carried by transformants was verified by Sanger sequencing. The insert cloned in the pDONR207 was subcloned into the pMDC32 Gateway-compatible destination vector (61) via an LR Clonase II (Thermo Fisher) reaction. The transgene was mobilized into *Agrobacterium tumefaciens* GV3101 (C58C1 Rif^{R}) cells and those were used to transform Col-0, *ipt9-1* and *ipt9-2* plants by the floral dipping (62). T_1 transgenic plants were selected on plates supplemented with 15 mg/L Hygromycin B (Duchefa).

Genome-wide identification of additional T-DNA insertions in KG7770

We sequenced the *ipt9-1* (KG7770) genome and followed a tagged-sequence strategy to map the potential additional insertions as described in (44). Briefly, 8.6 µg of nuclear-enriched DNA was purified from 0.5 g of *ipt9-1* seedlings as previously described in (63). Whole-genome sequencing of the sample was performed at BGI Hong Kong using a BGISEQ-500 sequencing platform. 28.93 million 150-bp-long reads were obtained, reaching a 32X genome depth. Trimmed fastq files were used to map the position of the insertion using Easymap software (64). Raw reads were deposited in Short Read Archive with the code SRX14238175.

RESULTS

Cytokinin deficient mutants display different primary root phenotypes

CK biosynthesis pathway can be blocked, in principle, in three different levels targeted by the mutants *ipt357* (2), *cypa1a2* (20) and *ipt29* (2). These three mutant lines are known for impaired iP-, *t*Z and *c*Z- biosynthesis, respectively (Figure 1A). CK's inhibitory effect in root growth has been well established (1) and most CK deficient and insensitive mutants display longer primary roots accordingly (65). Here, we have grown *ipt357*, *cypa1a2* and *ipt29* mutants for seven days and assessed their primary root growth. The mutants *ipt357* and *cypa1a2* displayed longer primary root phenotypes compared to Col-0 (Figure 1B-C) while *ipt29*, impaired in *c*Z production, exhibited a severely reduced root growth (Figure 1B-C). While this phenotype of *ipt29* has been previously described by other authors (19), it remains enigmatic. Therefore, here we aimed to elucidate the *ipt29* short-root mutant phenotype by using the *ipt357* and *cypa1a2* mutants as controls.

The primary root defect observed in *ipt29* mutant was consistent with shorter meristematic root zone size compared to Col-0 (Figure 1D-E) and its CK metabolic profile showed severely lower levels of *c*ZR and *c*Z but also of iP compared to wild type plants (Figure 1F). Both the *ipt357* and the *cypa1a2* mutants displayed lower contents for *t*Z riboside and *t*Z compared to Col-0, while iPR and iP levels were higher only in *cypa1a2* mutant (Figure 1F).

ipt29 short-root phenotype is cytokinin independent and is controlled by local signals

To assess whether exogenous CK supply could rescue the defective root phenotypes of these mutant lines, *ipt357*, *cypa1a2* and *ipt29* were grown for seven days in media supplemented with 100 nM iP, *t*Z or *c*Z. All three CK compounds inhibited root growth in all genotypes (Figure 2A). The inhibitory effect on root growth was similar for *t*Z and iP and lower for *c*Z both in the wild-type and all the mutant lines (Figure 2A-B). While the longer root phenotypes of *ipt357* and *cypa1a2* observed compared to Col-0 in mock conditions were inverted in response to CK treatments, the short root phenotype of *ipt29* still remained (Figure 2A). In fact, 100 nM cZ could fully rescue the *ipt357* and *cypa1a2* root phenotypes but not that of *ipt29* (Figure 2A). Similar results were observed in root growth elongation rate assays in which the same genotypes were grown for six days in MS media and then transferred for one day to media supplemented with 100 nM iP, *t*Z or *c*Z (Supplementary Figure 1A-B). None of these three active CKs could rescue the short-root phenotype of *ipt29* (Figure 2A), nor any of the *c*Z concentrations applied in the dose-response assay shown in Figure 2D.

Induction of CK responses following 100 nM iP, *t*Z and *c*Z treatment was assessed with fluorescence imaging of root tips from the CK response reporter line *TCSn:GFP*. All three CKs were able to induce CK signaling when seedlings were grown on treated media (Figure 2C) or when seedlings were transferred for 24 h to media containing the respective treatment (Supplementary Figure 1C). Both the *TCSn:GFP* and the transcriptional fusion of *ARABIDOPSIS THALIANA RESPONSE REGULATOR5* (*ARR5*) promoter to the β-glucuronidase (*ARR5*$_{pro}$*:GUS*) lines (55) displayed increased intensity of CK signaling in response to 24 h of different CK types, in the order: iP > *t*Z > *c*Z (Supplementary Figure 1C, D). Finally, comparing *ipt29* root phenotype with Col-0 when plants were grown for 14 days confirmed that the root remained significantly shorter in the mutant even after a longer growth period (Figure 2E).

The results obtained so far pinpointed that the *c*Z deficiency of the *ipt29* mutant most likely was not linked with the short-root phenotype, and therefore another non-CK signal could be the explanation. As a first step, we examined whether this signal was shoot-derived or local. To answer this, reciprocal grafts were performed between scions and rootstocks derived from Col-0 and *ipt29* genotypes, and grafts of the same genotype were used as controls, as shown in Figure 3A.

The grafts were performed when the plants were four-day-old and thereafter their root growth was recorded daily. As shown in Figure 3B, the control grafts Col-0/Col-0 (scion/rootstock) and *ipt29*/*ipt29* had the previously observed difference in primary root length (Figure 1B-C). The reciprocal grafts *ipt29*/Col-0 and Col-0/*ipt29* both displayed shorter roots compared to the wild type control graft. Since the Col-0 scion was not sufficient to restore the short-root phenotype of the *ipt29* rootstock (Figure 3B), we concluded that the signal controlling the phenotype is not shoot-derived and it is likely locally generated in root tissues.

A strong link was observed between auxin metabolism and the *ipt29* short-root phenotype

Our results so far indicated that the shorter root phenotype of the *ipt29* mutant is not CK-dependent and is controlled locally in the root tissue. Another signal that often interacts with CK to regulate root growth and can act locally is auxin (66,67). Therefore, we carried out a detailed profiling of auxin and related metabolites, analysing separately shoot and root tissues for the active form IAA as well as several precursors such as anthranilate (ANT), Trp, IPyA, and IAN, and inactive forms like indole-3-acetyl glutamate (IAA-Glu), 2-oxindole-3-acetic acid (oxIAA) or 2-oxoindole-3-acetyl-1-O-ß-D-glucose (oxIAA-glc) (Figure 4A, B). Both in shoot and root tissues,

IAA levels were significantly higher in *ipt29* than Col-0, this difference being more acute in root tissues. In shoots, IAA levels were slightly higher in *ipt29* compared to wild type, while all the inactive forms analysed were depleted. Regarding the precursors, ANT levels were reduced in *ipt29* while the others were indistinguishable from Col-0 (Figure 4A). In roots, IAA metabolism was more strikingly affected with higher levels of IAA inactivated catabolites, while among the precursors only Trp levels were significantly higher in *ipt29* than Col-0 (Figure 4B). The chlorotic phenotype of *ipt29* leaves suggests some type of chloroplast misfunction, pointing to a potential defect on the IAA precursor Trp. Our results, however, discard any Trp deficiency and rather discovered a clear link between the *ipt29* mutation and higher IAA levels. Overall effects of auxin on root growth are very concentration dependent: low concentrations of IAA normally promote growth, but altering IAA homeostasis and enhancing IAA concentrations results in growth inhibition, potentially explaining the *ipt29* root phenotype.

IPT9 is solely responsible for the *c*Z-independent *ipt29* phenotype

To ascertain whether there is a differential contribution to the *ipt29* phenotype from either of the two paralog genes, we analysed the primary root phenotype of both single mutants. Surprisingly, while *ipt2* single mutant root phenotype was indistinguishable from the wild type, *ipt9* roots were as short as those of the double *ipt29* (Figure 5A-B). We then wondered if levels of *c*ZR, *c*Z and IAA could explain these differential phenotypic contributions in the single mutants. However, concentrations of *c*ZR and *c*Z were much more reduced in *ipt2* than in *ipt9* roots, further confirming the CK-independence of the *ipt29* short root phenotype (Figure 5C). In line with the link found between the *ipt29* short root phenotype and IAA metabolism, *ipt9* showed higher IAA levels both in shoot and root while *ipt2* IAA levels were indistinguishable from Col-0 (Figure 4A, B).

Since all our analysis have been performed using previously reported T-DNA insertional mutants and it is well established that the average number of T-DNAs in insertional lines is greater than two (68), we wondered if an additional insertional event could explain the defects we observe in *ipt9*. To rule out this possibility, we sequenced the *ipt9* genome and followed a tagged-sequencing strategy to map the position of all the insertional events. We confirmed the presence of an insertion only in At5g20040 (*IPT9*; Supplemental Figure 2A). We also obtained a second insertional allele for *IPT9*, the line GK_302_F10 from the GABI-KAT collection. Therefore, we re-named the already published allele of *IPT9* (KG7770) as *ipt9-1*, and the GABI-KAT line as *ipt9-2*. The insertions interrupt the second (*ipt9-1*) and the eighth (*ipt9-2*) intron of the *IPT9* gene, both affecting the sequence coding for the tRNA delta(2)-isopentenylpyrophosphate transferase

protein domain (IPP; pfam01715; Figure 5D). We then performed a phenotypic complementation assay with both alleles. All homozygous and trans-heterozygous plants combining *ipt9* mutant alleles showed significantly shorter roots than Col-0, thus confirming the direct relationship between *IPT9* misfunction and the *ipt9* and *ipt29* short root phenotype (Figure 5E-F), among other phenotypic traits such as chlorotic leaves (Supplementary Figure 2B-D) and shorter stems (Supplementary Figure 2E-G). We next transferred a transgene containing a wild-type version of *IPT9* driven by cauliflower mosaic virus 35S promoter to both *ipt9-1* and *ipt9-2* mutant lines (Figure 5E, F, Supplementary Figure 3 A-C). Detailed analysis of multiple independent transgenic families (selected from different T_0 families) showed that not only in most of the transgenics the root phenotype was restored to wild-type levels but also that in some families, roots were even longer than Col-0 (Figure 5E, F, Supplementary Figure 3 A-C). To remove potential interactions between the wild type and the mutant version of IPT9 in any mutant background, we also introduced the transgene into Col-0 plants. Again, some families, 6 out of 10 analysed in detail, showed enhanced root growth compared to non-transgenic Col-0 (Supplemental Figure 3D, E). To explore the IAA metabolic landscape of these plants overexpressing *IPT9,* we performed auxin profiling of shoots and roots (Figure 4A, B). While in shoots the effects of this transgene increased the IAA levels even further, IAA levels in roots were the same as Col-0. Other differential shoot/root effects of the transgene such us the increased levels of ANT, Trp and IAA-Glu found in shoots were not mimicked in roots (Figure 4A,B). IPyA was the only exception, with higher levels in both tissues. In conclusion, our allelic and transgenic complementation combined with phenotypic and hormonal analyses demonstrated that mutations in the *IPT9* are wholly responsible for the *ipt29* short root phenotype.

DISCUSSION

CKs are important for plant development as they are regulating multiple plant functions. In contrast with other plant hormones, such as auxins or brassinosteroids, CKs have more than one active molecule. These are the nucleobases iP, *t*Z, *c*Z and dihydrozeatin. They can bind to CK receptors and initiate the corresponding hormonal responses affecting various physiological aspects of plant growth such as root growth, contributing thus to plant development and adaptation. These four molecules have different affinities to their receptors (6–8,69), they can be produced in same but also in spatially different locations within the plant tissues (19–21,70–80) and they are degraded and conjugated at different rates (9,81,82). It is thus interesting to understand why this hormone has four, instead of one, active molecules and whether these could possibly have different effects in specific plant functions, such as root growth.

The *ipt29* double mutant has a unique primary root phenotype

The triple and double mutants, *ipt357*, *cypa1a2* and *ipt29*, are inhibited in different parts of the CK iP, *t*Z and *c*Z biosynthesis pathways, respectively (Figure 1A). Previous studies have shown that *ipt357* has a longer primary root compared to wild type, supporting the inhibitory effect of CK on root growth (1) and our results show that this is also the case for the *cypa1a2* double mutant. Interestingly *ipt29*, specifically blocked *c*Z production, has shorter roots compared to wild type plants.

This intriguing phenotype that could potentially suggest that *c*Z has an opposite effect in root growth compared to the other active CK compounds, triggered not only our interest but also the one of Kollmer *et al* (19). In their work studying the *CKX7* gene, they found that CKX7 enzyme preferred *c*Z compounds as substrate compared to other CKs (9,19) and that plants that overexpressed *CKX7* had severely retarded root growth compared to wild type, similarly to *ipt29* root phenotype (19). Their results showed that *c*Z-CKs play an important, yet not exclusive, role in vascular differentiation as other CK-types could affect this process. However, the question of why the *ipt29* mutant has a shorter root phenotype remained unanswered.

Our results confirmed the defective primary root phenotype of *ipt29* in comparison with Col-0 and the other adenylate-*IPT* mutants that had longer primary roots (Figure 1B-C). The observed phenotypes were in accordance with shorter and longer meristematic zone of the mutants' roots, respectively (Figure 1D-E). The correspondence of root meristem size and primary root length of *ipt29* mutant is in agreement with previous findings (19).

Initially, we compared the CK profiles between 7-day-old Col-0 and the CK-type deficient mutants. The results overall confirmed the expected reduced CK-types content in the respective mutant. In addition, the higher concentration of *t*Z and *t*ZR in *ipt357* and the reciprocal effect of higher CK iP-type and lower *t*Z-type levels in *cypa1a2* mutant roots, suggested that in young Arabidopsis roots most of the iPMRP produced by IPT action is converted into *t*ZRMP for *t*Z-rypes production. This supports the importance of *t*Z in Arabidopsis young roots in agreement with this compound's prevalence in CK responsive cells of the same plant and tissue (29). In *ipt29* mutant roots, *c*Z-CKs concentrations were severely reduced as previously shown in older plants (2,19). Based on the reduced concentration of iP in *ipt29* and the increased *c*Z levels in *ipt357* mutants, an enigmatic hypothesis could be a potential enzymatic connection between iP and *c*Z biosynthesis pathways.

cZ deficiency is not linked with the *ipt29* short-root phenotype

All active CK molecules (iP, *t*Z, *c*Z) were able to suppress the increased root growth (Figure 2A-B) and growth rate (Sup. Fig 1A-B) phenotypes of *ipt357* and *cypa1a2,* indicating that the longer root phenotypes in these mutants are caused by CK deficiency. These experiments (Figure 2A, B and Supplementary Figure 1A-B) also revealed that *c*Z has the weakest effect on root length and growth rate compared to the other two active CKs applied (*t*Z~iP>>*c*Z), implying that cZ could have a less important role in root growth regulation compared to the other two compounds. Although actual embryos have not been examined, embryonic effects seem unlikely to be the cause of the *ipt29* phenotype because of the following results. Firstly, the seeds of *ipt29* germinated at the same time as Col-0. Secondly, *ipt29* mutants grown for the longer period of 14 days displayed the same retarded root growth compared to the wild type as the 7-day-old seedlings (Figure 2E). Finally, the *ipt29* root defects could be also attributed to the lower root growth rate of this mutant (Supplementary Figure 1A-B) which is a post-embryonic process. Overall, since no applied concentration of *c*Z (Figure 2D) and no other CK treatment (Figure 2A) could alter the retarded root growth or elongation of *ipt29* mutant, it can be concluded that inhibition of root growth in *ipt29* mutant is a CK-independent phenotype.

In fact, when *c*Z was applied exogenously the root phenotype of *ipt357* and *cypa1a2* could be fully rescued (Figure 2A and Supplementary Figure 1A-B). This supports that *c*Z acts as an inhibitor of root growth, like the other active CKs, possibly following binding of *c*Z to AHK CK receptors and thus activating downstream signaling. Indeed, *c*Z treatment was able to activate the CK response reporter line, *TCSn:GFP* (28), although in lower intensity compared to iP and *t*Z (Figure 2C and Supplementary Figure 1C). It has been previously shown that CK receptors differ in their preference of CK isoforms (6,83,84) and Lomin et al, summarized in their review data supporting that *c*Z has lower affinity to AHK receptors compared to iP and *t*Z in both Arabidopsis and maize (85).

An alternative scenario for the *c*Z-driven responses mentioned above that cannot be excluded is that *c*Z, at least partially, converts to *t*Z via potential isomerization by zeatin cis-/trans-isomerase as shown in maize cultures. When these were incubated for 20 min with *c*Z, about one tenth of the compound was converted to *t*Z (8). Another explanation in our case could be that *c*Z conversion into *t*Z occurs via the hydroxylation of N6-isopentenyl side chain or other unknown reaction. In parallel, feeding experiments on Arabidopsis protoplasts and maize cultured cells with labelled *c*Z indicated to a metabolic route from *c*Z not only to respective conjugates but also back to its precursor forms (8,29). However, in such feeding experiments on rice seedlings, tobacco cells, oat leaves and Arabidopsis protoplasts no isomerization was observed between *t*Z- and *c*Z-ribosides (9,14,86). Likewise, lack of isomerization from *t*Z to *c*Z was inferred from absence of

detectable *c*Z-types in the *ipt29* double mutant (2). The above studies suggest that *c*Z-type levels are pivotally controlled by *de novo* *c*Z-biosynthesis through the tRNA pathway. Lack of *cis-trans* isomerization also indicates that the high levels of *c*ZR being transported through the plant body (26) are more likely to have a biological role directly as *c*ZR or *c*Z rather than contributing to the *t*Z- CK pools of the sink.

The *ipt29* mutant phenotype is governed by local signals in the root

Previous grafting experiments have revealed that CKs can act not only as local signals but also as distal ones. Interestingly, *c*Z-types and more specifically *c*ZR are prevalent compounds in phloem and xylem sap of Arabidopsis (26) although this compound seems to be almost inactive when tested *in vitro* receptor binding assays in Arabidopsis and maize (7,8). In agreement, *c*ZR was unable to initiate ARR5-mediated CK response (7). On the other hand, *c*ZR had strong effect in tobacco callus growth and oat chlorophyll retention bioassays (9). This indicates that *c*ZR can have great activity in bioassays probably after its conversion to the bioactive *c*Z. Transport of cZ CKs in inactive forms such as *c*ZR could provide a further regulatory level to control extent of CK responses.

Shoot-born CKs can act as an inhibitory signal of nodule formation on *Lotus japonicus* roots (87). The defective phenotype of *ipt1357* quadrupole mutant scion and rootstock could be restored by Col-0 rootstock and scion in reciprocal grafting experiments (23). Also, *cypa1a2* shoot phenotype was rescued when the mutant scion was merged with wild type rootstock (20). To verify that *ipt29* sort root phenotype is unrelated to endogenously transported CKs, grafting experiments were performed (Figure 3). Shoot-derived CKs from Col-0 scion were unable to restore the *ipt29* rootstock phenotype (Figure 3B) suggesting that the signal controlling this phenotype is a local signal in the root and according to our results it is not CK-dependent.

Link to auxin metabolism and differential contribution of *ipt2* and *ipt9* to the short root phenotype

Auxin and CKs have been previously shown to interact at many levels such as biosynthesis, signalling and transport controlling several developmental processes including lateral root initiation, vascular development and meristem size and maintenance (88). Examples of CK-auxin crosstalk include the SUPPRESSOR OF HYPOCOTYL2 (SHY2), which controls root meristem activity by balancing auxin and CK responses. While the SKP1-CULLIN1-F-BOX (SCF)–TRANSPORT INHIBITOR RESISTANT1 (SCF^{TIR1}) complex enables the auxin-dependent degradation of SHY2 (47,48), B-RRs-regulated CK signaling in the root meristem transition zone,

directly activates *SHY2* transcription. SHY2 then negatively affects auxin efflux and response. In addition, SHY2 also induces CK biosynthesis by upregulation of *IPT5* (49,50) Interaction of the two hormones also control the activity of the quiescent center (QC). In fact, ARR1-dependent CK signaling causes downregulation of the auxin influx carrier *LIKE AUXIN RESISTANT2* (*LAX2*), leading to attenuation of auxin response and division in QC cells (51). In the QC, the transcription factor SCARECROW (SCR) suppresses ARR1 and affects auxin biosynthesis (52). Auxin also antagonizes CK by direct transcriptional activation of *ARR7* and *ARR15* that are repressors of CK signaling (53). A domain of high-auxin signaling in the xylem cells and a domain of high-CK signaling in the procambium and phloem cell lineages is described to control vascular tissue patterning. Very recently, auxin was found to activate the TARGET OF MONOPTEROS 5 and LONESOME HIGHWAY (TMO5/LHW) heterodimer complex that serves as central organizer for vascular development and patterning in the root apical meristem. The TMO5/LHW module, in turn, directly controls SHORTROOT (SHR) to balance CK levels (54).

Auxin was thus a good candidate signal to assess as a potential explanation for the *ipt29* phenotype, since it can act in the root to regulate growth and development in crosstalk with CKs. IAA exhibited higher abundance compared to wild type in the short-root *ipt29* mutant (Figure 4A). This correlated with increases of IAA inactive forms such as oxIAA, oxIAA-glc, and IAA-Glu (Figure 4B). The link between auxin metabolism and the shorter root phenotype was further examined in the *ipt2* and *ipt9* single mutants. The short-root phenotype and altered IAA levels of *ipt29* were maintained only by the *ipt9* mutation and not by *ipt2* which showed wild type primary root growth and IAA levels (Figure 4 and 5). The concentration of *c*ZR and *c*Z in the roots of *ipt2* were reduced as severely as in *ipt29* compared to Col-0, while the depletion was much less pronounced in *ipt9* roots (Figure 5C). This result in combination with the phenotype of the root confirms our previous finding that the short root phenotype of *ipt9* and *ipt29* are not dependent on *c*Z concentration. In contrast, IAA content was elevated exclusively in the plants with short-root phenotypes (Figure 4) confirming the link between auxin and the phenotype in question.

We further carefully evaluated the connexion between lesions in *IPT9* and the root phenotypes. After confirming that there were no additional insertions in the original *ipt9* mutant, we isolated a new allele for this gene showing very similar phenotypic traits. Complementation analyses confirmed the connection between mutations in *IPT9* and the observed phenotypes, further supported by transgenic plants expressing a wild-type version of *IPT9* in both mutant backgrounds. Intriguingly, many of the independent overexpressor lines had roots even longer than those of Col-0. Further research is required to elucidate the potential quantitative effects of *IPT9* transcript levels on root length. Overall, our work indicates that the *IPT9* gene is essential

529 for primary root growth. Although this gene is involved in biosynthesis of *c*Z-CKs, we hypothesize
530 that IPT9 could be functioning through manipulation of local auxin concentration in order to control
531 root growth.

FIGURE LEGENDS

Figure 1. **Mutants in different cytokinin biosynthetic genes show differential effects on primary root length and meristem size**. (A) Simplified version of the parallel cytokinin biosynthesis pathways. (B, C) Primary root phenotype and length quantification of the wild-type Col-0, the triple mutant *ipt357*, and the double mutants *cyp753a1 cyp753a2* (*cypa1a2*) and *ipt29*. (D, E) Root meristem phenotype and size quantification of the assorted genotypes. (F) Quantification of some biologically active cytokinins in the assorted genotypes expressed as picomoles per 100 roots. Pictures were taken 7 days after stratification (das). Scale bars indicate (B) 1 cm, and (D) 100 µm. Asterisks indicate values significantly different from Col-0 in a (C, E) Student' *t* test and (D) Mann-Whitney *U* test (*p<0.05, **p<0.01, ***p<0.001, ****p<0.0001; n≥ (C) 13, (E) 24, (F) 6). ADP/ATP, adenosine di/triphosphate; DMAPP, dimethylallyl diphosphate; tRNA, transferTransfer ribonucleic acid; IPT, isopentenyltransferase; iPR, isopentenyladenosine; *c*ZR, *cis*-zeatin riboside; *t*ZR, *trans*-zeatin riboside; iP, isopentenyladenine; *t*Z, *trans*-zeatin; *c*Z, *cis*-zeatin.

Figure 2. Mutants in different cytokinin biosynthetic genes show differential effects on primary root length and meristem size. (A) Primary root length of the wild-type Col-0, and the *ipt357*, *cypa1a2*, and *ipt29* multiple mutants grown for 7 days in media supplemented with 100 nM of iP, *t*Z and *c*Z. Black asterisks indicate values significantly different from Col-0 mock treatment and colour asterisks indicate significant differences from the corresponding mock genotype in a One-way ANOVA test (***p<0.001, ****p<0.0001; n ≥ 13). (B) Root growth inhibitory effects of iP, *t*Z and *c*Z on the genotypes mentioned in (A). (C) Cytokinin signalling reporter TCSn response to different cytokinin treatments. (D) *c*Z dose-response treatment of Col-0 and the ipt29 double mutant. Primary root length after 7 days growing in media supplemented with different *c*Z concentrations. Dots indicate average ± SD of at least 20 seedlings (E).

Figure 3. *ipt29* phenotype is mainly controlled by local signals. (A) Schematics representing grafting experiments performed between Col-0 and *ipt29* shoot and root. Col-0 and *ipt29* were self-grafted as controls. (B) Primary root growth of grafted seedlings. Dots indicate the average ± s.e.m. of the primary root length (n=24) of grafted and self-grafted seedlings of the assorted genotypes.

Figure 4 . Shoot and root profiling of auxin metabolites in cZ biosynthetic mutants. Anthranilate (ANT), Tryptophan (Trp), indole-3-pyruvic acid (IPyA), indole-3- acetonitrile (IAN), indole-3-acetic acid (IAA), 2-oxindole-3-acetic acid (oxIAA), 2-oxoindole-3-acetyl-1-O-ß-D-acetic acid glucose (oxIAA-glc), and indole-3-acetyl glutamateacetic acid glutamic (IAA-Glu) levels were quantified in (A) aerial tissues and (B) roots of Col-0, ipt29, ipt2, ipt9, $35S_{pro}$:IPT9 7-days-old seedlings. Concentrations are expressed in picomols per g of fresh weight. Error bars indicate standard error and asterisks indicate values significantly different from Col-0 in a Student's t test (* p <0.05, ** p <0.01, *** p <0.001, **** p <0.0001; n ≥ 4).

Figure 5. Lesions in *IPT9* are solely responsible of the *ipt29* phenotype and are *cZ*-independent. (A, B) Primary root phenotype (A) and length quantification (B) of Col-0, *ipt2*, *ipt9*, and *ipt29*. Asterisks indicate values significantly different from Col-0 in a Student's t test (* p <0.05, ** p <0.01, *** p <0.001, **** p <0.0001; n=5). (C) *c*ZR and *c*Z quantification of shoot and root of Col-0, *ipt2*, *ipt9*, and *ipt29*. (D) Structure of the *IPT9* gene and protein with the nature and positions of the *ipt9* mutations indicated. Boxes and lines represent exons and introns, respectively. Open and coloured boxes represent untranslated and translated regions, respectively. Triangles indicate T-DNA insertions in *ipt9-1* and *ipt9-2* mutants. Greenish shadowed regions represent exons encoding and region of the protein corresponding to the tRNA delta(2)-

582 isopentenylpyrophosphate transferase (IPP; pfam01715) domain. (E, F) Primary root phenotype
583 (E) and length quantification (F) of Col-0, homozygous *ipt9-1*, and *ipt9-2*, trans-heterozygous *ipt9-*
584 *1/ipt9-2*, and *ipt9-2/ipt9-1*, and transgenic plants in the *ipt9-1* background expressing *IPT9* under
585 the constitutive 35S promoter. Different letters indicate values significantly different ($p < 0.05$; n
586 of each population is indicated above the genotype) in a Tukey's post-doc test. Pictures were
587 taken (A, E) at 7 days. Scale bars indicate (A, E) 1 cm, (D) 0.5 kb and 100 amino acids.
588

Acknowledgements

We thank NASC for providing the plant lines used in this work and Roger Granbom (UPSC, Umeå, Sweden) for technical assistance. The Microscopy Platform of UPSC, the Swedish Metabolomics Centre and Plant Sciences Core Facility of CEITEC Masaryk University are acknowledged for their technical support. The work was funded by the European Molecular Biology Organization (EMBO short term fellowship, project 7034) (MP). KL acknowledge Sweden's Innovation Agency (Vinnova 2016-00504), the Knut and Alice Wallenberg Foundation (KAW 2016.0341 and KAW 2016.0352), the Swedish Research Council (VR 2018-04235) and Kempestiftelserna (JCK-2711 and JCK-1811). The Ministry of Education, Youth and Sports of the Czech Republic founded the work via the European Regional Development Fund-Project 'Plants as a tool for sustainable global development' (CZ.02.1.01/0.0/0.0/16_019/0000827) (ON, KD, AP, MK) and project "MSCAfellow@MUNI" [CZ.02.2.69/0.0/0.0/17_050/0008496] (MP).

Author contributions

I.A., O.N. and M.P. conceived the project; I.A., M.A. and M.P. performed the phenotypic, treatment and confocal experiments; O.N., A.P. I.A., M.P, F.B., M.K., K.D., E. M.-B. and A.A. conducted the purification and quantification of auxins and cytokinins; E. M.-B. performed the genetic analysis, cloning and phenotyping; M.-G.V., I.A. and C.T. discussed and performed the grafting experiment. I.A., E. M.-B., M.P. and O.N. analysed and interpreted the data; I.A. and E. M.-B. made the Figures; I.A. prepared the manuscript draft; I.A., E. M.-B., and K.L. wrote the paper with input from all authors.

Author Information

ORCID IDs:
Ioanna Antoniadi: 0000-0001-9053-2788
Eduardo Mateo-Bonmatí: 0000-0002-2364-5173
Markéta Pernisová: 0000-0002-5803-2879
Federica Brunoni: 0000-0003-1497-9419
Anita Ament: 0000-0001-5563-7330
Michal Karády: 0000-0002-5603-706X
Colin Turnbull: 0000-0001-6635-1418
Karel Doležal0000000349380350
Ales Pěnčík: 0000-0002-1314-2249
Karin Ljung: 0000-0003-2901-189X
Ondrej Novák: 0000-0003-3452-0154

SUPPORTING INFORMATION

Supplementary Figure 1: 24 h treatment with different CKs inhibit root growth and trigger CK signalling reporters *TCSn:GFP* and *ARR5$_{pro}$:GUS*.
Supplementary Figure 2: Insertion number analysis performed in *ipt9-1* and shoot phenotypes of the *ipt9* mutants.
Supplementary Figure 3: Root phenotypic effects of the *35S$_{pro}$:IPT9* transgene in mutant and wild-type backgrounds.
Supplementary Table 1: Primer sets used in this work

635 **References**

636 1. Stenlid G. Cytokinins as inhibitors of root growth. Physiol Plant. 1982;56(4):500–6.

637 2. Miyawaki K, Tarkowski P, Matsumoto-Kitano M, Kato T, Sato S, Tarkowska D, et al.
638 Roles of Arabidopsis ATP/ADP isopentenyltransferases and tRNA
639 isopentenyltransferases in cytokinin biosynthesis. Proc Natl Acad Sci U S A [Internet].
640 2006 Oct 31;103(44):16598–603. Available from:
641 http://www.pubmedcentral.nih.gov/articlerender.fcgi?artid=1637627&tool=pmcentrez&ren
642 dertype=abstract

643 3. Schmitz RY, Skoog F, Playtis a. J, Leonard NJ. Cytokinins: synthesis and biological
644 activity of geometric and position isomers of zeatin. Plant Physiol [Internet]. 1972 Dec
645 1;50(6):702–5. Available from:
646 http://www.pubmedcentral.nih.gov/articlerender.fcgi?artid=366220&tool=pmcentrez&rend
647 ertype=abstract

648 4. Kamínek M, Vaněk T, Motyka V. Cytokinin activities of N6-benzyladenosine derivatives
649 hydroxylated on the side-chain phenyl ring. J Plant Growth Regul. 1987;6(2):113–20.

650 5. Inoue T, Higuchi M, Hashimoto Y, Seki M, Kobayashi M, Kato T, et al. Identi ® cation of
651 CRE1 as a cytokinin receptor from Arabidopsis. Nature. 2001;409(6823):1060–3.

652 6. Romanov G a, Lomin SN, Schmülling T. Biochemical characteristics and ligand-binding
653 properties of Arabidopsis cytokinin receptor AHK3 compared to CRE1/AHK4 as revealed
654 by a direct binding assay. J Exp Bot [Internet]. 2006 Jan [cited 2014 Mar 7];57(15):4051–
655 8. Available from: http://www.ncbi.nlm.nih.gov/pubmed/17075078

656 7. Spíchal L, Rakova NY, Riefler M, Mizuno T, Romanov G a, Strnad M, et al. Two cytokinin
657 receptors of Arabidopsis thaliana, CRE1/AHK4 and AHK3, differ in their ligand specificity
658 in a bacterial assay. Plant Cell Physiol [Internet]. 2004 Sep;45(9):1299–305. Available
659 from: http://www.ncbi.nlm.nih.gov/pubmed/15509853

660 8. Yonekura-sakakibara K, Kojima M, Yamaya T, Sakakibara H. Molecular Characterization
661 of Cytokinin-Responsive Histidine Kinases in Maize . Differential Ligand Preferences and
662 Response to cis-Zeatin 1. Plant Physiol. 2004;134(4):1654–61.

663 9. Gajdosová S, Spíchal L, Kamínek M, Hoyerová K, Novák O, Dobrev PI, et al. Distribution,
664 biological activities, metabolism, and the conceivable function of cis-zeatin-type
665 cytokinins in plants. J Exp Bot [Internet]. 2011 May [cited 2014 Aug 28];62(8):2827–40.
666 Available from: http://www.ncbi.nlm.nih.gov/pubmed/21282330

667 10. Emery JRN, Leport L, Barton JE, Turner NC, Atkins CA, Agriculture M. cis-Isomers of
668 Cytokinins Predominate in Chickpea Seeds throughout Their Development 1. Plant
669 Physiol. 1998;117:1515–23.

670 11. Veach YK, Martin RC, Mok DWS, Malbeck J, Vankova R, Mok MC. O-Glucosylation of
671 cis-Zeatin in Maize . Characterization of Genes , Enzymes , and Endogenous Cytokinins
672 1. Plant P. 2003;131:1374–80.

673 12. Kojima M, Kamada-Nobusada T, Komatsu H, Takei K, Kuroha T, Mizutani M, et al. Highly
674 sensitive and high-throughput analysis of plant hormones using MS-probe modification
675 and liquid chromatography-tandem mass spectrometry: an application for hormone
676 profiling in Oryza sativa. Plant Cell Physiol [Internet]. 2009 Jul [cited 2014 Aug
677 28];50(7):1201–14. Available from:

http://www.pubmedcentral.nih.gov/articlerender.fcgi?artid=2709547&tool=pmcentrez&rendertype=abstract

13. Quesnelle PE, Emery RJN. cis -Cytokinins that predominate in Pisum sativum during early embryogenesis will accelerate embryo growth in vitro. Can J Bot. 2007;85:9–103.

14. Kudo T, Makita N, Kojima M, Tokunaga H, Sakakibara H. Cytokinin Activity of cis-Zeatin and Phenotypic Alterations Induced by Overexpression of Putative cis-Zeatin-O-glucosyltransferase in Rice. Plant Physiol [Internet]. 2012 Sep [cited 2012 Sep 6];160(1):319–31. Available from: http://www.ncbi.nlm.nih.gov/pubmed/22811434

15. Vyroubalová S, Václavíková K, Turecková V, Novák O, Smehilová M, Hluska T, et al. Characterization of new maize genes putatively involved in cytokinin metabolism and their expression during osmotic stress in relation to cytokinin levels. Plant Physiol [Internet]. 2009 Sep [cited 2014 Sep 29];151(1):433–47. Available from: http://www.pubmedcentral.nih.gov/articlerender.fcgi?artid=2735981&tool=pmcentrez&rendertype=abstract

16. Havlová M, Dobrev PI, Motyka V, Storchová H, Libus J, Dobrá J, et al. The role of cytokinins in responses to water deficit in tobacco plants over-expressing trans-zeatin O-glucosyltransferase gene under 35S or SAG12 promoters. Plant Cell Environ [Internet]. 2008 Mar [cited 2014 Sep 29];31(3):341–53. Available from: http://www.ncbi.nlm.nih.gov/pubmed/18088334

17. Dobra J, Motyka V, Dobrev P, Malbeck J, Prasil IT, Haisel D, et al. Comparison of hormonal responses to heat, drought and combined stress in tobacco plants with elevated proline content. J Plant Physiol [Internet]. 2010 Nov 1 [cited 2014 Sep 11];167(16):1360–70. Available from: http://www.ncbi.nlm.nih.gov/pubmed/20619485

18. Pertry I, Václavíková K, Depuydt S, Galuszka P, Spíchal L, Temmerman W, et al. Identification of Rhodococcus fascians cytokinins and their modus operandi to reshape the plant. Proc Natl Acad Sci U S A [Internet]. 2009 Jan 20;106(3):929–34. Available from: http://www.pubmedcentral.nih.gov/articlerender.fcgi?artid=2630087&tool=pmcentrez&rendertype=abstract

19. Köllmer I, Novák O, Strnad M, Schmülling T, Werner T. Overexpression of the cytosolic cytokinin oxidase/dehydrogenase (CKX7) from Arabidopsis causes specific changes in root growth and xylem differentiation. Plant J [Internet]. 2014 Feb 17 [cited 2014 Mar 27];1–13. Available from: http://www.ncbi.nlm.nih.gov/pubmed/24528491

20. Kiba T, Takei K, Kojima M, Sakakibara H. Side-chain modification of cytokinins controls shoot growth in Arabidopsis. Dev Cell [Internet]. 2013 Nov 25 [cited 2014 May 3];27(4):452–61. Available from: http://www.ncbi.nlm.nih.gov/pubmed/24286826

21. Takei K, Yamaya T, Sakakibara H. Arabidopsis CYP735A1 and CYP735A2 encode cytokinin hydroxylases that catalyze the biosynthesis of trans-Zeatin. J Biol Chem [Internet]. 2004 Oct 1 [cited 2012 Jul 17];279(40):41866–72. Available from: http://www.ncbi.nlm.nih.gov/pubmed/15280363

22. Sakakibara H. Cytokinins: activity, biosynthesis, and translocation. Annu Rev Plant Biol [Internet]. 2006 Jan [cited 2012 Jul 27];57:431–49. Available from: http://www.ncbi.nlm.nih.gov/pubmed/16669769

23. Matsumoto-Kitano M, Kusumoto T, Tarkowski P, Kinoshita-Tsujimura K, Václavíková K,

Miyawaki K, et al. Cytokinins are central regulators of cambial activity. Proc Natl Acad Sci U S A [Internet]. 2008 Dec 16;105(50):20027–31. Available from: http://www.pubmedcentral.nih.gov/articlerender.fcgi?artid=2605004&tool=pmcentrez&rendertype=abstract

24. Ko D, Kang J, Kiba T, Park J, Kojima M, Do J, et al. Arabidopsis ABCG14 is essential for the root-to-shoot translocation of cytokinin. Proc Natl Acad Sci U S A [Internet]. 2014 Apr 28 [cited 2014 May 5];111(19):7150–5. Available from: http://www.pubmedcentral.nih.gov/articlerender.fcgi?artid=4024864&tool=pmcentrez&rendertype=abstract

25. Zhang K, Novak O, Wei Z, Gou M, Zhang X, Yu Y, et al. Arabidopsis ABCG14 protein controls the acropetal translocation of root-synthesized cytokinins. Nat Commun [Internet]. 2014 Feb 11 [cited 2014 Feb 12];5:3274. Available from: http://www.ncbi.nlm.nih.gov/pubmed/24513716

26. Hirose N, Takei K, Kuroha T, Kamada-Nobusada T, Hayashi H, Sakakibara H. Regulation of cytokinin biosynthesis, compartmentalization and translocation. J Exp Bot [Internet]. 2008 Jan [cited 2012 Jul 15];59(1):75–83. Available from: http://www.ncbi.nlm.nih.gov/pubmed/17872922

27. Kieber JJ, Schaller GE. Cytokinin signaling in plant development. Development [Internet]. 2018;145(4):1–7. Available from: http://dev.biologists.org/lookup/doi/10.1242/dev.149344

28. Zürcher E, Tavor-Deslex D, Lituiev D, Enkeli K, Tarr PT, Müller B. A robust and sensitive synthetic sensor to monitor the transcriptional output of the cytokinin signaling network in planta. Plant Physiol [Internet]. 2013 Jan 25 [cited 2013 Mar 1];161(3):1066–75. Available from: http://www.ncbi.nlm.nih.gov/pubmed/23355633

29. Antoniadi I, Novák O, Gelová Z, Johnson A, Plíhal O, Simerský R, et al. Cell-surface receptors enable perception of extracellular cytokinins. Nat Commun [Internet]. 2020 Dec 1 [cited 2021 Apr 12];11(1):1–10. Available from: https://doi.org/10.1038/s41467-020-17700-9

30. Casanova-Sáez R, Mateo-Bonmatí E, Ljung K. Auxin metabolism in plants. Cold Spring Harb Perspect Med. 2021;11(3):1–23.

31. Stepanova AN, Robertson-Hoyt J, Yun J, Benavente LM, Xie DY, Doležal K, et al. TAA1-Mediated Auxin Biosynthesis Is Essential for Hormone Crosstalk and Plant Development. Cell. 2008;133(1):177–91.

32. Tao Y, Ferrer JL, Ljung K, Pojer F, Hong F, Long JA, et al. Rapid Synthesis of Auxin via a New Tryptophan-Dependent Pathway Is Required for Shade Avoidance in Plants. Cell. 2008;133(1):164–76.

33. Yamada M, Greenham K, Prigge MJ, Jensen PJ, Estelle M. The TRANSPORT INHIBITOR RESPONSE2 Gene is required for auxin synthesis and diverse aspects of plant development. Plant Physiol. 2009;151(1):168–79.

34. Mashiguchi K, Tanaka K, Sakai T, Sugawara S, Kawaide H, Natsume M, et al. The main auxin biosynthesis pathway in Arabidopsis. Proc Natl Acad Sci U S A. 2011;108(45):18512–7.

35. Stepanova AN, Yun J, Robles LM, Novak O, He W, Guo H, et al. The Arabidopsis YUCCA1 Flavin Monooxygenase functions in the Indole-3-Pyruvic acid branch of Auxin

765 Biosynthesis. Plant Cell. 2011;23(11):3961–73.

766 36. Won C, Shen X, Mashiguchi K, Zheng Z, Dai X, Cheng Y, et al. Conversion of tryptophan
767 to indole-3-acetic acid by tryptophan aminotransferases of Arabidopsis and YUCCAs in
768 Arabidopsis. Proc Natl Acad Sci U S A. 2011;108(45):18518–23.

769 37. Hull AK, Vij R, Celenza JL. Arabidopsis cytochrome P450s that catalyze the first step of
770 tryptophan-dependent indole-3-acetic acid biosynthesis. Proc Natl Acad Sci U S A.
771 2000;97(5):2379–84.

772 38. Mikkelsen MD, Hansen CH, Wittstock U, Halkier BA. Cytochrome P450 CYP79B2 from
773 Arabidopsis catalyzes the conversion of tryptophan to indole-3-acetaldoxime, a precursor
774 of indole glucosinolates and indole-3-acetic acid. J Biol Chem. 2000;275(43):33712–7.

775 39. Zhao Y, Hull AK, Gupta NR, Goss KA, Alonso J, Ecker JR, et al. Trp-dependent auxin
776 biosynthesis in Arabidopsis: Involvement of cytochrome P450s CYP79B2 and CYP79B3.
777 Genes Dev. 2002;16(23):3100–12.

778 40. Pollmann S, Neu D, Weiler EW. Molecular cloning and characterization of an amidase
779 from Arabidopsis thaliana capable of converting indole-3-acetamide into the plant growth
780 hormone, indole-3-acetic acid. Phytochemistry. 2003;62(3):293–300.

781 41. Sánchez-Parra B, Frerigmann H, Alonso MMP, Loba VC, Jost R, Hentrich M, et al.
782 Characterization of four bifunctional plant IAM/PAM-amidohydrolases capable of
783 contributing to auxin biosynthesis. Plants. 2014;3(3):324–47.

784 42. Mateo-Bonmatí E, Casanova-Sáez R, Šimura J, Ljung K. Broadening the roles of UDP-
785 glycosyltransferases in auxin homeostasis and plant development. New Phytol.
786 2021;232(2):642–54.

787 43. Staswick PE, Serban B, Rowe M, Tiryaki I, Maldonado MT, Maldonado MC, et al.
788 Characterization of an arabidopsis enzyme family that conjugates amino acids to indole-
789 3-acetic acid. Plant Cell. 2005;17(2):616–27.

790 44. Casanova-Sáez R, Mateo-Bonmatí E, Šimura J, Pěnčík A, Novák O, Staswick P, et al.
791 Inactivation of the entire Arabidopsis group II GH3s confers tolerance to salinity and
792 water deficit. New Phytologist. 2022. 0–3 p.

793 45. Müller K, Dobrev PI, Pencík A, Hosek P, Vondráková Z, Filepová R, et al. Dioxygenase
794 for auxin oxidation 1 catalyzes the oxidation of IAA amino acid conjugates. Plant Physiol.
795 2021;187(1):103–15.

796 46. Porco S, Pěnčík A, Rasheda A, Vo U, Casanova-Sáez R, Bishopp A, et al. Dioxygenase-
797 encoding AtDAO1 gene controls IAA oxidation and homeostasis in arabidopsis. Proc Natl
798 Acad Sci U S A. 2016;113(39):11016–21.

799 47. Dharmasiri N, Dharmasiri S, Jones AM, Estelle M. Auxin Action in a Cell-Free System.
800 Curr Biol CB Biol. 2003;13:1418–22.

801 48. Tian Q, Uhlir NJ, Reed JW. Arabidopsis SHY2 / IAA3 Inhibits Auxin-Regulated Gene
802 Expression. 2002;14(February):301–19.

803 49. Dello Ioio R, Nakamura K, Moubayidin L, Perilli S, Taniguchi M, Morita MT, et al. A
804 genetic framework for the control of cell division and differentiation in the root meristem.
805 Science [Internet]. 2008 Nov 28;322(5906):1380–4. Available from:
806 http://www.ncbi.nlm.nih.gov/pubmed/19039136

50. Moubayidin L, Perilli S, Dello Ioio R, Di Mambro R, Costantino P, Sabatini S. The rate of cell differentiation controls the arabidopsis root meristem growth phase. Curr Biol [Internet]. 2010;20(12):1138–43. Available from: http://dx.doi.org/10.1016/j.cub.2010.05.035

51. Zhang W, Swarup R, Bennett M, Schaller GE, Kieber JJ. Cytokinin induces cell division in the quiescent center of the Arabidopsis root apical meristem. Curr Biol [Internet]. 2013 Oct 21 [cited 2014 Mar 20];23(20):1979–89. Available from: http://www.ncbi.nlm.nih.gov/pubmed/24120642

52. Moubayidin L, Di Mambro R, Sozzani R, Pacifici E, Salvi E, Terpstra I, et al. Spatial coordination between stem cell activity and cell differentiation in the root meristem. Dev Cell [Internet]. 2013 Aug 26 [cited 2014 Oct 15];26(4):405–15. Available from: http://www.ncbi.nlm.nih.gov/pubmed/23987513

53. Müller B, Sheen J. Cytokinin and auxin interplay in root stem-cell specification during early embryogenesis. Nature [Internet]. 2008 Jun 19 [cited 2013 Mar 7];453(7198):1094–7. Available from: http://www.pubmedcentral.nih.gov/articlerender.fcgi?artid=2601652&tool=pmcentrez&rendertype=abstract

54. Yang BJ, Minne M, Brunoni F, Plačková L, Petřík I, Sun Y, et al. Non-cell autonomous and spatiotemporal signalling from a tissue organizer orchestrates root vascular development. Nat Plants. 2021;7(11):1485–94.

55. Che P, Gingerich DJ, Lall S, Howell SH. Global and Hormone-Induced Gene Expression Changes during Shoot Development in Arabidopsis. 2002;14(November):2771–85.

56. Schindelin J, Arganda-carreras I, Frise E, Kaynig V, Longair M, Pietzsch T, et al. Fiji : an open-source platform for biological-image analysis. Nat Methods. 2012;9(7):676–82.

57. Malamy JE, Benfey PN. Organization and cell differentiation in lateral roots of Arabidopsis thaliana. Development. 1997;124:33–44.

58. Svačinová J, Novák O, Plačková L, Lenobel RR, Holík J, Strnad M, et al. A new approach for cytokinin isolation from Arabidopsis tissues using miniaturized purification: pipette tip solid-phase extraction. Plant Methods [Internet]. 2012 Jan 17 [cited 2012 Sep 7];8(1):17. Available from: http://www.ncbi.nlm.nih.gov/pubmed/22594941

59. Pěnčík A, Casanova-Sáez R, Pilařová V, Žukauskaite A, Pinto R, Micol JL, et al. Ultra-rapid auxin metabolite profiling for high-throughput mutant screening in Arabidopsis. J Exp Bot. 2018;69(10):2569–79.

60. Turnbull CGN, Booker JP, Leyser HMO. Micrografting techniques for testing long-distance signalling in Arabidopsis. Plant J [Internet]. 2002 Oct;32(2):255–62. Available from: http://www.ncbi.nlm.nih.gov/pubmed/12383090

61. Curtis MD, Grossniklaus U. A Gateway Cloning Vector Set for High-Throughput Functional Analysis of Genes in Planta. Plant Physiol. 2003;133(2):462–9.

62. Clough SJ, Bent AF. Floral dip: A simplified method for Agrobacterium-mediated transformation of Arabidopsis thaliana. Plant J. 1998;16(6):735–43.

63. Hanania U, Velcheva M, Sahar N, Perl A. An Improved Method for Isolating High-Quality DNA From Vitis vinifera Nuclei. Plant Mol Biol Report. 2004;22:173–7.

64. Lup SD, Wilson-sánchez D, Andreu-sánchez S. Easymap : A User-Friendly Software Package for Rapid Mapping-by-Sequencing of Point Mutations and Large Insertions. 2021;12(May):1–10.

65. Argyros RD, Mathews DE, Chiang Y-H, Palmer CM, Thibault DM, Etheridge N, et al. Type B response regulators of Arabidopsis play key roles in cytokinin signaling and plant development. Plant Cell [Internet]. 2008 Aug [cited 2014 Sep 7];20(8):2102–16. Available from: http://www.pubmedcentral.nih.gov/articlerender.fcgi?artid=2553617&tool=pmcentrez&rendertype=abstract

66. Su Y-H, Liu Y-B, Zhang X-S. Auxin-cytokinin interaction regulates meristem development. Mol Plant [Internet]. 2011 Jul [cited 2012 Jul 18];4(4):616–25. Available from: http://www.pubmedcentral.nih.gov/articlerender.fcgi?artid=3146736&tool=pmcentrez&rendertype=abstract

67. Brumos J, Robles LM, Yun J, Vu TC, Jackson S, Alonso JM, et al. Local Auxin Biosynthesis Is a Key Regulator of Plant Article Local Auxin Biosynthesis Is a Key Regulator of Plant Development. Dev Cell [Internet]. 2018;47(3):306-318.e5. Available from: https://doi.org/10.1016/j.devcel.2018.09.022

68. Wilson-Sánchez D, Rubio-Díaz S, Muñoz-Viana R, Pérez-Pérez JM, Jover-Gil S, Ponce MR, et al. Leaf phenomics: A systematic reverse genetic screen for Arabidopsis leaf mutants. Plant J. 2014;79(5):878–91.

69. Schwartzenberg K von, Núñez MF, Blaschke H, Dobrev PI, Novák O, Motyka V, et al. Cytokinins in the bryophyte Physcomitrella patens: analyses of activity, distribution, and cytokinin oxidase/dehydrogenase overexpression reveal the role of extracellular cytokinins. Plant Physiol [Internet]. 2007 Dec [cited 2014 Aug 31];145(3):786–800. Available from: http://www.pubmedcentral.nih.gov/articlerender.fcgi?artid=2048801&tool=pmcentrez&rendertype=abstract

70. Kiba T, Yamada H, Sato S, Kato T, Tabata S, Mizuno T. The Type-A Response Regulator , ARR15 , Acts as a Negative Regulator in the Cytokinin-Mediated Signal Transduction in Arabidopsis thaliana. 2003;44(8):868–74.

71. Kiba T, Yamada H, Mizuno T. Characterization of the ARR15 and ARR16 response regulators with special reference to the cytokinin signaling pathway mediated by the AHK4 histidine kinase in roots of Arabidopsis thaliana. Plant Cell Physiol [Internet]. 2002 Sep;43(9):1059–66. Available from: http://www.ncbi.nlm.nih.gov/pubmed/12354925

72. To JPC, Haberer G, Ferreira FJ, Derue J, Schaller GE, Alonso JM, et al. Type-A Arabidopsis Response Regulators Are Partially Redundant Negative Regulators of Cytokinin Signaling. 2004;16(March):658–71.

73. To JPC, Deruère J, Maxwell BB, Morris VF, Hutchison CE, Ferreira FJ, et al. Cytokinin regulates type-A Arabidopsis Response Regulator activity and protein stability via two-component phosphorelay. Plant Cell [Internet]. 2007 Dec [cited 2012 Jul 17];19(12):3901–14. Available from: http://www.pubmedcentral.nih.gov/articlerender.fcgi?artid=2217641&tool=pmcentrez&rendertype=abstract

74. Tanaka Y, Suzuki T, Yamashino T, Mizuno T. Comparative Studies of the AHP Histidine-

containing Phosphotransmitters Implicated in His-to-Asp Phosphorelay in Arabidopsis thaliana. 2004;68(2):462–5.

75. Miyawaki K, Matsumoto-Kitano M, Kakimoto T. Expression of cytokinin biosynthetic isopentenyltransferase genes in Arabidopsis : tissue specificity and regulation by auxin, cytokinin, and nitrate. Plant J [Internet]. 2004 Jan [cited 2012 Jul 23];37(1):128–38. Available from: http://doi.wiley.com/10.1046/j.1365-313X.2003.01945.x

76. Kuroha T, Tokunaga H, Kojima M, Ueda N, Ishida T, Nagawa S, et al. Functional analyses of LONELY GUY cytokinin-activating enzymes reveal the importance of the direct activation pathway in Arabidopsis. Plant Cell [Internet]. 2009 Oct [cited 2012 Jul 13];21(10):3152–69. Available from: http://www.pubmedcentral.nih.gov/articlerender.fcgi?artid=2782294&tool=pmcentrez&rendertype=abstract

77. Werner T, Motyka V, Laucou V, Smets R, Onckelen H Van, Thomas S. Cytokinin-Deficient Transgenic Arabidopsis Plants Show Functions of Cytokinins in the Regulation of Shoot and Root Meristem Activity. Plant Cell. 2003;15(11):2532–50.

78. Nishimura C, Ohashi Y, Sato S, Kato T, Tabata S, Ueguchi C. Histidine Kinase Homologs That Act as Cytokinin Receptors Possess Overlapping Functions in the Regulation of Shoot and Root Growth in Arabidopsis. Plant Cell. 2004;16(6):1365–77.

79. Higuchi M, Pischke MS, Miyawaki K, Hashimoto Y, Seki M, Mahonen AP, et al. In planta functions of the Arabidopsis cytokinin receptor family. PNAS. 2004;101(23):8821–6.

80. D'Agostino IB, Deruère J, Kieber JJ. Characterization of the response of the Arabidopsis response regulator gene family to cytokinin. Plant Physiol [Internet]. 2000 Dec;124(4):1706–17. Available from: http://www.pubmedcentral.nih.gov/articlerender.fcgi?artid=59868&tool=pmcentrez&rendertype=abstract

81. Kowalska M, Galuszka P, Frébortová J, Šebela M, Béres T, Hluska T, et al. Vacuolar and cytosolic cytokinin dehydrogenases of Arabidopsis thaliana: heterologous expression, purification and properties. Phytochemistry [Internet]. 2010 Dec [cited 2014 Sep 2];71(17–18):1970–8. Available from: http://www.ncbi.nlm.nih.gov/pubmed/20825956

82. Galuszka P, Popelková H, Werner T, Frébortová J, Pospíšilová H, Mik V, et al. Biochemical Characterization of Cytokinin Oxidases/Dehydrogenases from Arabidopsis thaliana Expressed in Nicotiana tabacum L. J Plant Growth Regul [Internet]. 2007 Aug 21 [cited 2012 Nov 10];26(3):255–67. Available from: http://www.springerlink.com/index/10.1007/s00344-007-9008-5

83. Lomin SN, Yonekura-Sakakibara K, Romanov GA, Sakakibara H. Ligand-binding properties and subcellular localization of maize cytokinin receptors. J Exp Bot. 2011;62(14):5149–59.

84. Stolz A, Riefler M, Lomin SN, Achazi K, Romanov G a, Schmülling T. The specificity of cytokinin signalling in Arabidopsis thaliana is mediated by differing ligand affinities and expression profiles of the receptors. Plant J [Internet]. 2011 Jul [cited 2012 Jul 31];67(1):157–68. Available from: http://www.ncbi.nlm.nih.gov/pubmed/21426428

85. Lomin SN, Krivosheev DM, Steklov MY, Osolodkin DI, Romanov G a. Receptor properties and features of cytokinin signaling. Acta Naturae [Internet]. 2012 Jul;4(3):31–45. Available from:

http://www.pubmedcentral.nih.gov/articlerender.fcgi?artid=3491891&tool=pmcentrez&rendertype=abstract

86. Antoniadi I, Plačková L, Simonovik B, Doležal K, Turnbull C, Ljung K, et al. Cell-Type-Specific Cytokinin Distribution within the Arabidopsis Primary Root Apex. Plant Cell [Internet]. 2015;27(7):1955–67. Available from: http://www.plantcell.org/lookup/doi/10.1105/tpc.15.00176

87. Sasaki T, Suzaki T, Soyano T, Kojima M, Sakakibara H, Kawaguchi M. Shoot-derived cytokinins systemically regulate root nodulation. Nat Commun [Internet]. 2014 Sep 19 [cited 2014 Sep 19];5:4983. Available from: http://www.nature.com/doifinder/10.1038/ncomms5983

88. Bishopp A, Benková E, Helariutta Y. Sending mixed messages: Auxin-cytokinin crosstalk in roots. Curr Opin Plant Biol. 2011;14(1):10–6.

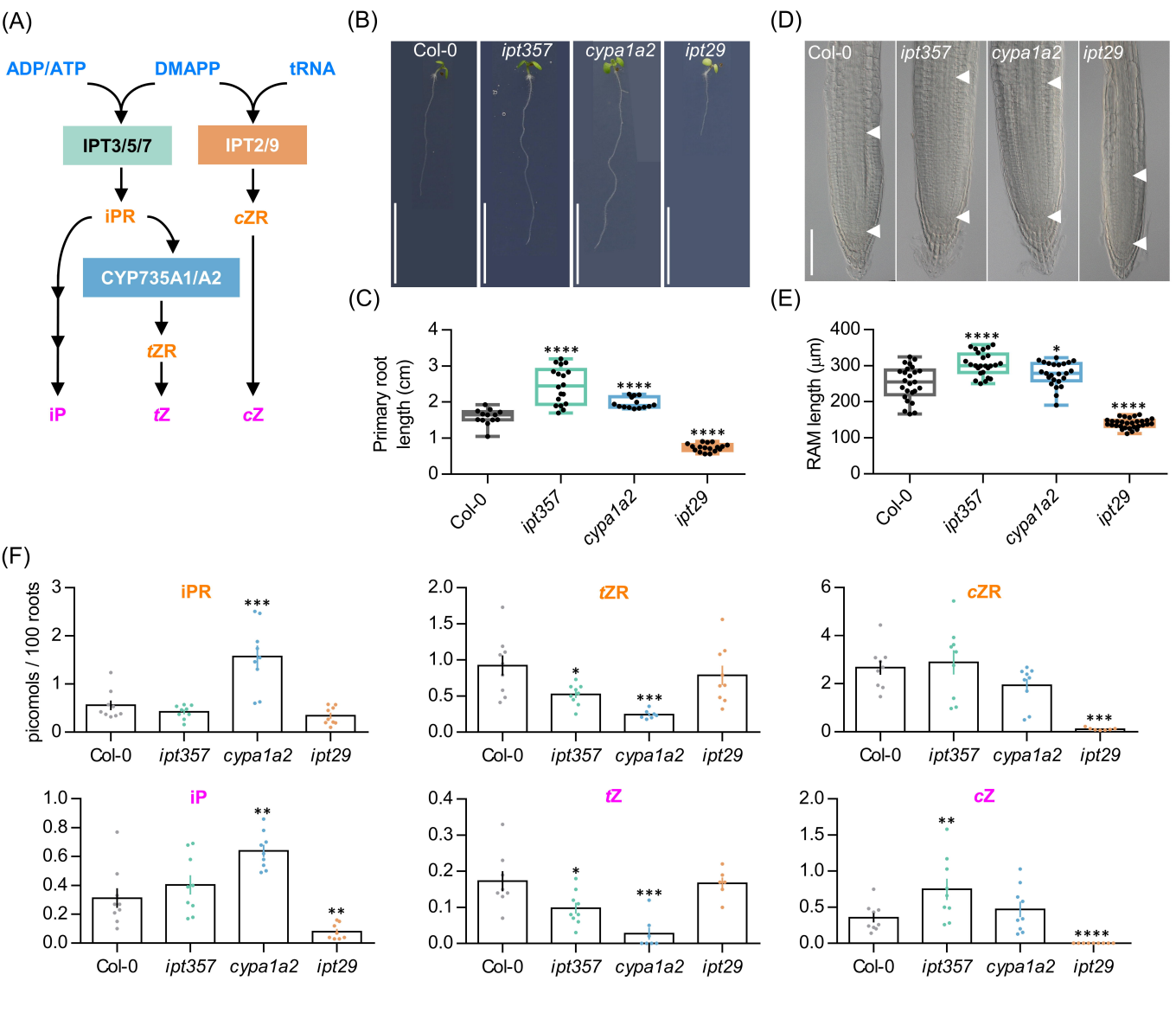
(A)
ADP/ATP
DMAPP
tRNA
IPT3/5/7
IPT2/9
iPR
cZR
CYP735A1/A2
tZR
iP
tZ
cZ
(B)
Col-0
ipt357
cypa1a2
ipt29
(D)
Col-0
ipt357
cypa1a2
ipt29
(C)
Primary root length (cm)
****
****
****
Col-0
ipt357
cypa1a2
ipt29
(E)
RAM length (µm)
****
*
****
Col-0
ipt357
cypa1a2
ipt29
(F)
picomols / 100 roots
iPR
***
tZR
*
***
cZR
***
iP
**
**
tZ
*
***
cZ
**
****
Col-0
ipt357
cypa1a2
ipt29

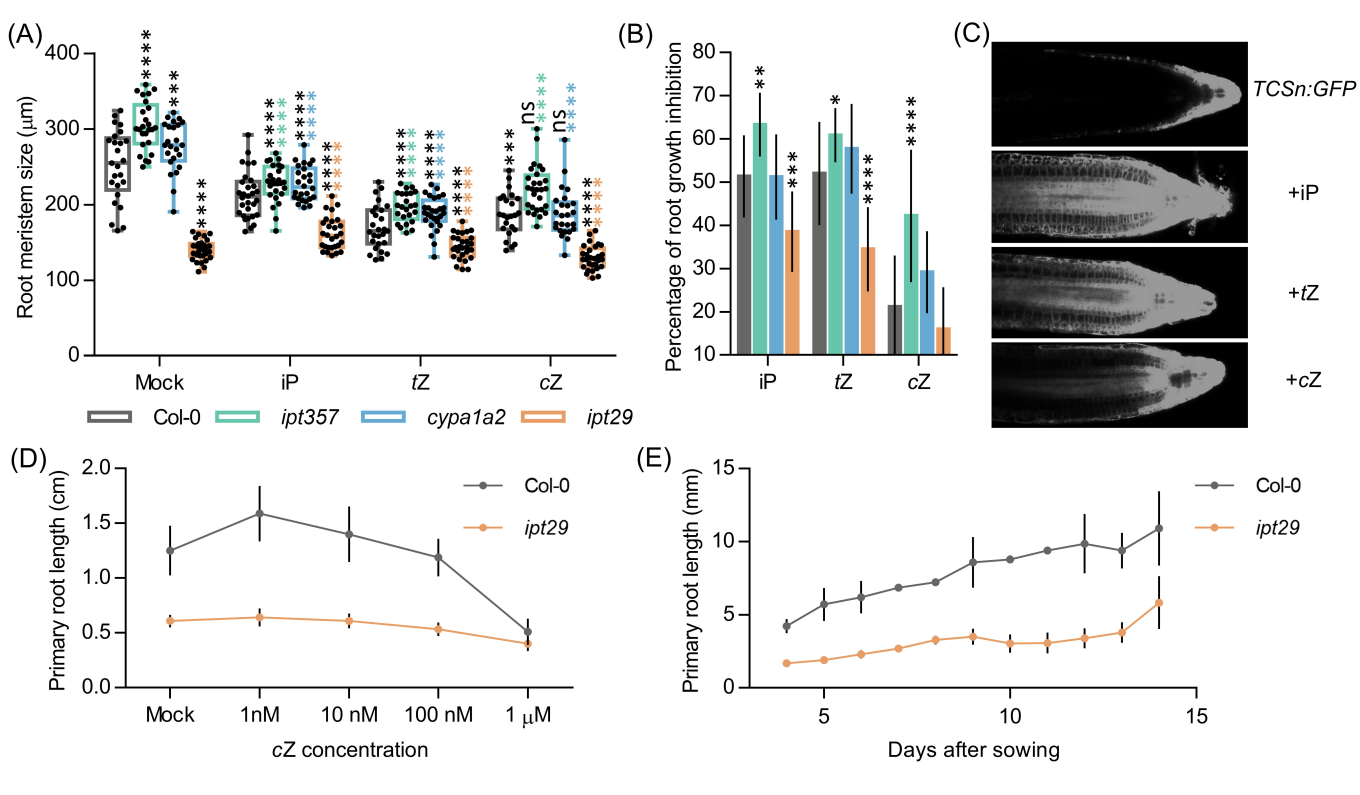
(A)
Root meristem size (μm)
400
300
200
100
0
Mock
iP
tZ
cZ
Col-0
ipt357
cypa1a2
ipt29
(B)
Percentage of root growth inhibition
80
70
60
50
40
30
20
10
iP
tZ
cZ
(C)
TCSn:GFP
+iP
+tZ
+cZ
(D)
Primary root length (cm)
2.0
1.5
1.0
0.5
0.0
Col-0
ipt29
Mock
1nM
10 nM
100 nM
1 μM
cZ concentration
(E)
Primary root length (mm)
15
10
5
0
Col-0
ipt29
5
10
15
Days after sowing

(A)

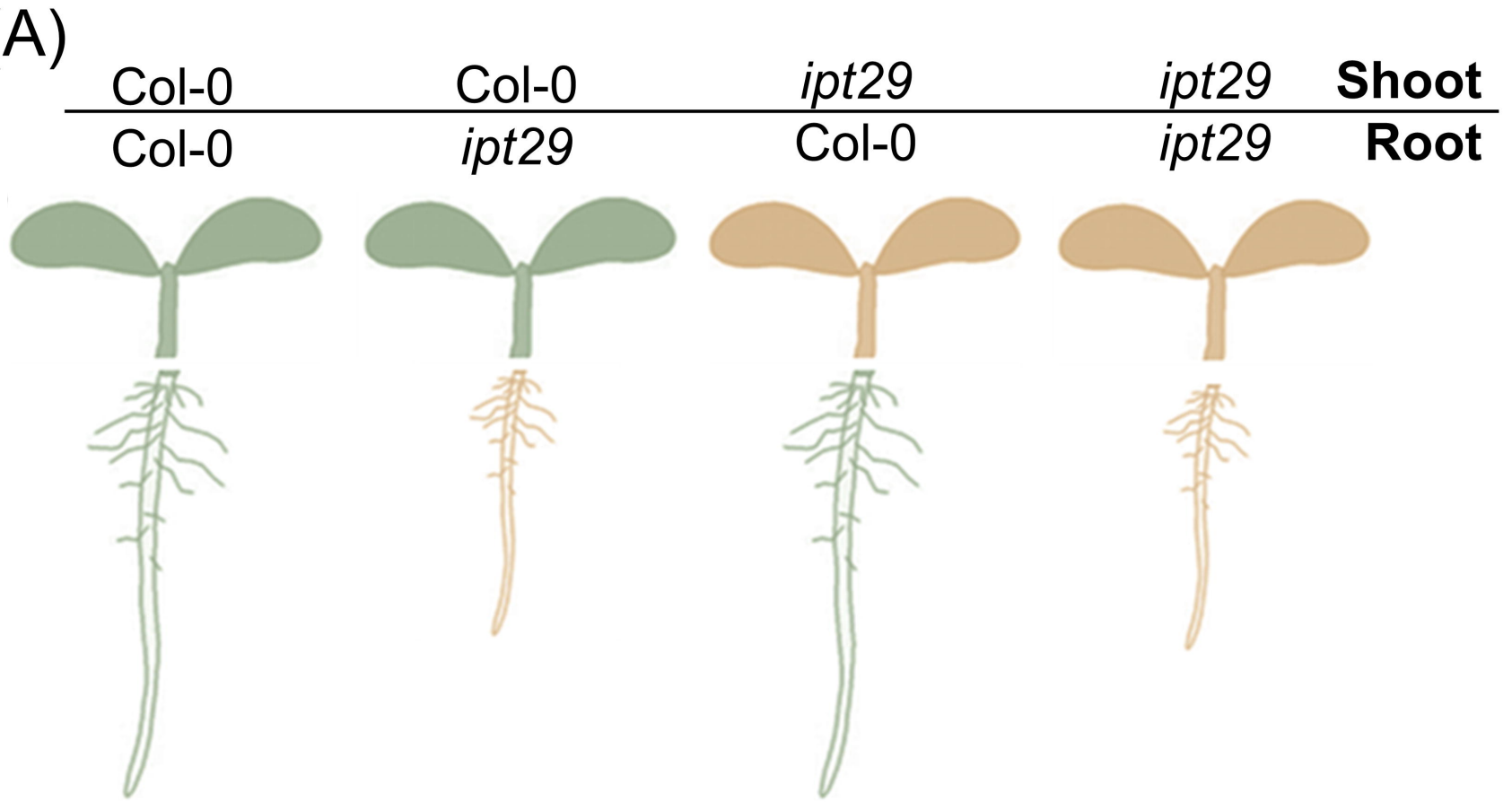
Col-0
Col-0
ipt29
ipt29
Shoot
Col-0
ipt29
Col-0
ipt29
Root

(B)

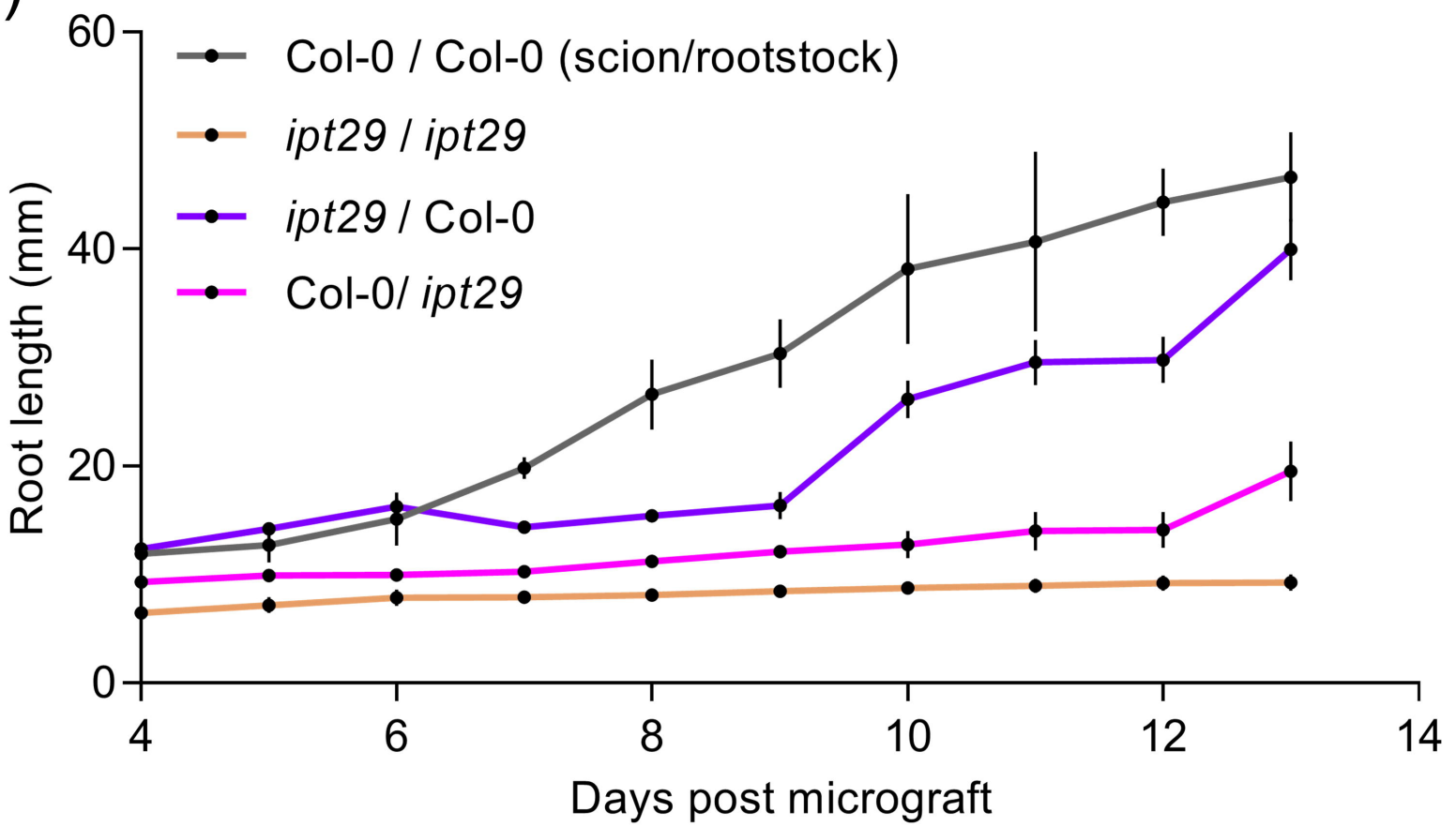
Col-0 / Col-0 (scion/rootstock)
ipt29 / ipt29
ipt29 / Col-0
Col-0/ ipt29
Root length (mm)
0
20
40
60
4
6
8
10
12
14
Days post micrograft

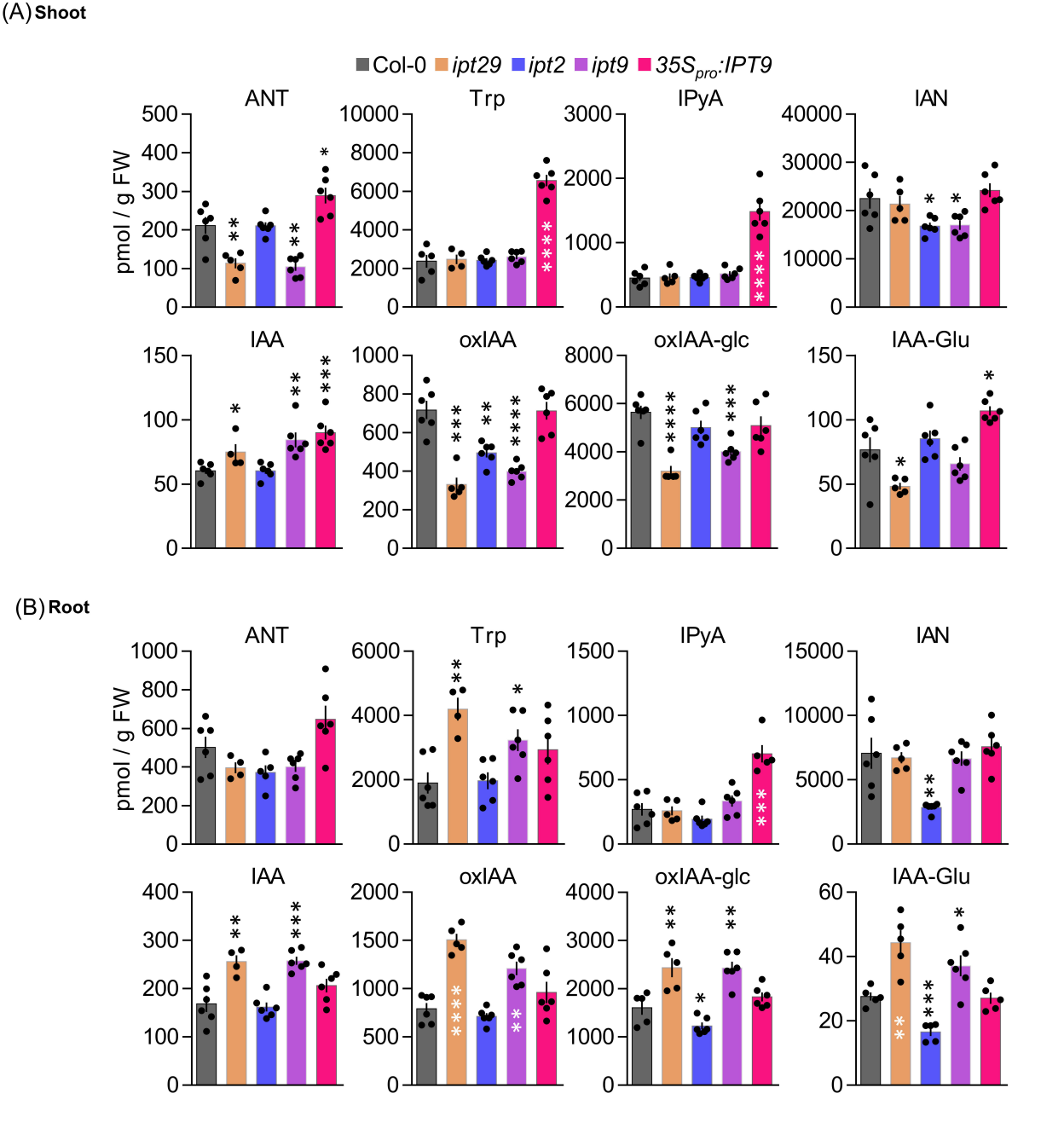
(A) Shoot
Col-0
ipt29
ipt2
ipt9
35S_pro:IPT9
ANT
Trp
IPyA
IAN
IAA
oxIAA
oxIAA-glc
IAA-Glu
pmol / g FW
(B) Root
ANT
Trp
IPyA
IAN
IAA
oxIAA
oxIAA-glc
IAA-Glu
pmol / g FW

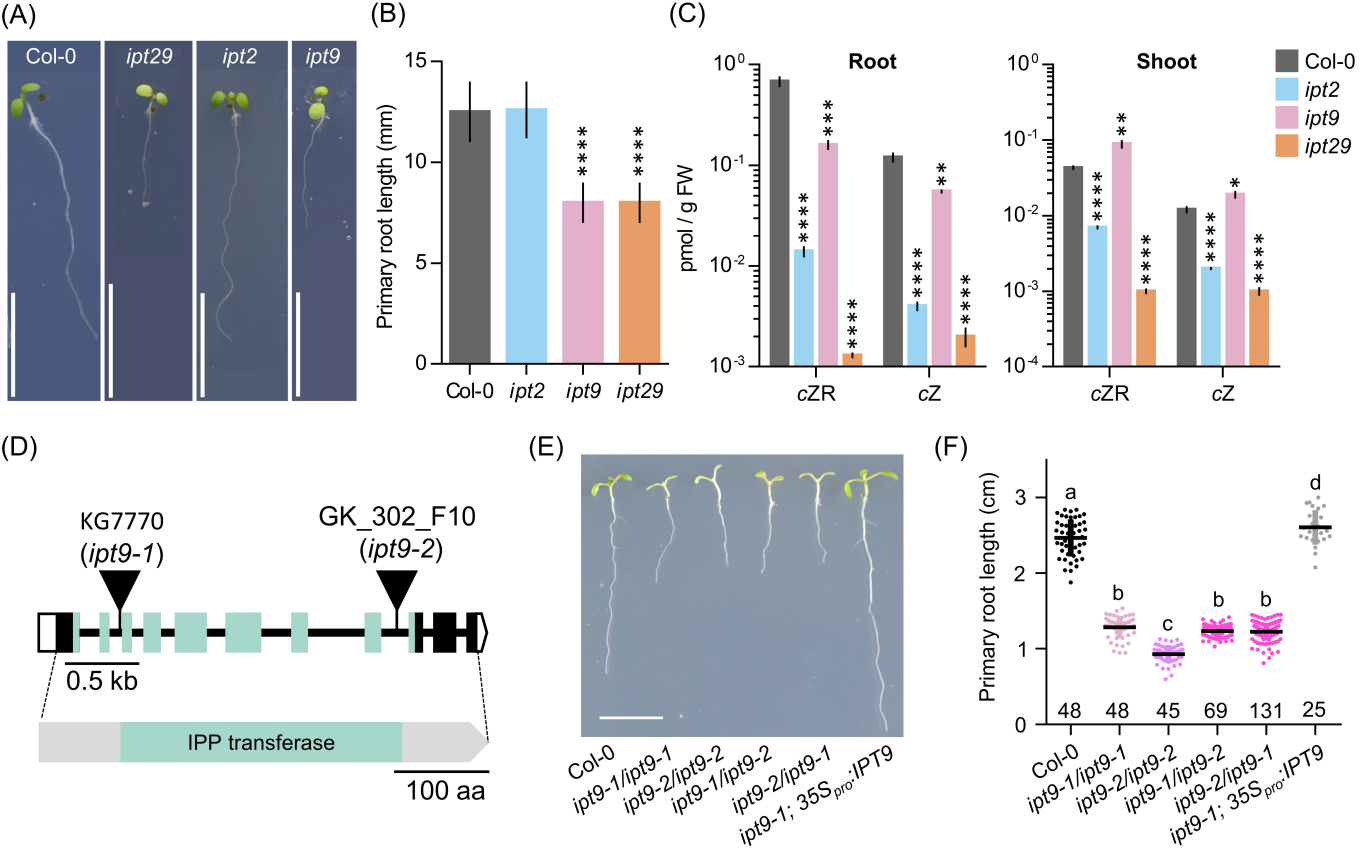
(A)
Col-0
ipt29
ipt2
ipt9
(B)
Primary root length (mm)
15
10
5
0
Col-0
ipt2
ipt9
ipt29
(C)
Root
Shoot
pmol / g FW
cZR
cZ
Col-0
ipt2
ipt9
ipt29
(D)
KG7770
(ipt9-1)
GK_302_F10
(ipt9-2)
0.5 kb
IPP transferase
100 aa
(E)
Col-0
ipt9-1/ipt9-1
ipt9-2/ipt9-2
ipt9-1/ipt9-2
ipt9-2/ipt9-1
ipt9-1; 35S pro:IPT9
(F)
Primary root length (cm)
a
b
c
b
b
d
48
48
45
69
131
25
Col-0
ipt9-1/ipt9-1
ipt9-2/ipt9-2
ipt9-1/ipt9-2
ipt9-2/ipt9-1
ipt9-1; 35S pro:IPT9